



Article

Metabolic Profiling of Organic Acids Reveals the Involvement of *HuIPMS2* in Citramalic Acid Synthesis in Pitaya

Jiaxuan Chen ^{1,†}, Yuanju Yuan ^{1,2,†}, Fangfang Xie ¹, Zhike Zhang ¹, Jianye Chen ¹, Rong Zhang ¹, Jietang Zhao ¹, Guibing Hu ¹ and Yonghua Qin ^{1,*}

- ¹ Guangdong Provincial Key Laboratory of Postharvest Science of Fruits and Vegetables/Key Laboratory of Biology and Genetic Improvement of Horticultural Crops (South China), Ministry of Agriculture and Rural Affairs, College of Horticulture, South China Agricultural University, Guangzhou 510642, China; jxchen0127@163.com (J.C.); yyj974028200@163.com (Y.Y.); xiefangfang202012@163.com (F.X.); poloky2@163.com (Z.Z.); chenjianye@scau.edu.cn (J.C.); r-zhang@scau.edu.cn (R.Z.); zhaojietang@gmail.com (J.Z.); guibing@scau.edu.cn (G.H.)
- ² Zhanjiang Research Center, Institute of Nanfan & Seed Industry, Guangdong Academy of Sciences, Zhanjiang 524300, China
- * Correspondence: qinyh@scau.edu.cn
- † These authors contribute equally to this work.



Citation: Chen, J.; Yuan, Y.; Xie, F.; Zhang, Z.; Chen, J.; Zhang, R.; Zhao, J.; Hu, G.; Qin, Y. Metabolic Profiling of Organic Acids Reveals the Involvement of *HuIPMS2* in Citramalic Acid Synthesis in Pitaya. *Horticulturae* **2022**, *8*, 167. <https://doi.org/10.3390/horticulturae8020167>

Academic Editor: Tiaobao Yang

Received: 11 December 2021

Accepted: 14 February 2022

Published: 16 February 2022

Publisher's Note: MDPI stays neutral with regard to jurisdictional claims in published maps and institutional affiliations.



Copyright: © 2022 by the authors. Licensee MDPI, Basel, Switzerland. This article is an open access article distributed under the terms and conditions of the Creative Commons Attribution (CC BY) license (<https://creativecommons.org/licenses/by/4.0/>).

Abstract: Pitayas are rich in organic acids, especially citramalic acid, which is significantly higher than the plants. However, the mechanism of citramalic acid biosynthesis remains to be fully elucidated. In this study, organic acid compositions and contents, as well as expression patterns of key genes related to organic acid metabolism were analyzed during fruit maturation of four different pitaya cultivars i.e., ‘Guanhuabai’ (GHB), ‘Guanhuahong’ (GHH), ‘Wucihuanglong’ (WCHL), and ‘Youcihuanglong’ (YCHL). The total organic acid contents increased first and then declined during fruit maturation. The main organic acids were citramalic acid during the early stages of GHB, GHH, and WCHL pitayas, and dominated by malic acid as fruit maturation. In comparison, citric acid and malic acid were main organic acid for ‘YCHL’ pitaya. Citramalate synthase (IPMS) was involved in the synthesis of citramalic acid, and three types of *HuIPMS* i.e., *HuIPMS1*, *HuIPMS2*, and *HuIPMS3*, were obtained in our study. Highest expression levels of *HuIPMS1* were detected in sepals, while *HuIPMS2* and *HuIPMS3* exhibited preferential expression in tender stems and ovaries. The expression levels of *HuIPMS2* and *HuIPMS3* were positively correlated with the content of citramalic acid in the four pitaya cultivars. *HuIPMS2* was a chloroplast-localized protein, while *HuIPMS3* presented a cytoplasmic-like and nuclear subcellular localization. These findings provide an important basis for further understanding of the molecular mechanism that leads to citramalic acid metabolism during pitaya fruit maturation.

Keywords: fruit quality; pitaya; citramalic acid; expression analyses; *HuIPMS2*; citramalate synthase

1. Introduction

Organic acids are important components of fruit flavor and nutritional quality which plays key roles in digestion and appetite. The types and ratios of organic acid components are responsible for fruit sourness and taste, and their differences contribute to unique flavors. Organic acids participate in the tricarboxylic acid cycle (TCA) and amino acid metabolism, and are further converted into sugars and esters [1]. The content of organic acids is usually higher in the early stages of fruit development, and is consumed as a respiratory substrate during fruit ripening [2]. Citric acid and malic acid are the main types of organic acids in most fruits [3,4]. The organic acid metabolism of fruits is relatively complex, involving a multi-enzyme system such as citrate synthase (CS, EC 4.1.3.7), aconitase (ACO, EC 4.2.1.3), NAD-isocitrate dehydrogenase (NAD-IDH, EC 1.1.1.41), NAD-malate

dehydrogenase (NAD-MDH, EC 1.1.1.37), malate synthetase (MS, EC 4.1.3.2), phosphoenolpyruvate carboxylase (PEPC, EC 4.1.1.31), and NADP-malic enzyme (NADP-ME, EC 1.1.1.40) [3,5].

Citramalic acid (citramalate), an uncommon organic acid in plants, was first discovered in apple peel in 1953 [6]. Citramalic acid is derived from acetyl-CoA and pyruvate with a condensation reaction catalyzed by citramalate synthase (IPMS/CIMA, EC 4.1.3.22) both in plants and bacteria [7,8], or through the methylation of malic acid [9]. The first CIMA was cloned from *Methanocaldococcus jannaschii*, which is likely involved in the biosynthesis of isoleucine [10]. Citramalic acid serves as a five-carbon precursor for the chemical synthesis of methacrylic acid. It can be converted into methacrylic acid by catalytic decarboxylation and dehydration reactions [11], which can be polymerized into polymer materials which are widely used in the manufacture of building materials and medical equipment [12–15]. Citramalic acid can also be used as a suitable raw material for pharmaceutical production to synthesize 15-deoxy-16(S)-hydroxy-16-prostaglandin [16]. In the food industry, citramalic acid is used as an acidulant for soft drinks and production of citraconic acid [17]. High citramalic acid concentration is responsible for the unique sensory properties of industrial sake brewed with the *Km67* yeast strain [18]. However, the pathway of citramalic acid synthesis remains to be fully elucidated.

Pitaya (pitahaya or dragon fruit) belonging to the genus *Hylocereus* or *Selenicereus* of the Cactaceae family, originates from North, Central, and South America [19]. It is rich in dietary fiber, proteins, vitamins, minerals, organic acids, polyphenols, and betalains [20]. Citramalic acid was identified for the first time in the pulp of *Hylocereus* species [21]. Citramalic acid is the main organic acid with high content at the early fruit development stage of pitaya, suggesting the possibility of pitaya to become a natural source of citramalic acid [22]. However, no information is available about citramalic acid synthesis in pitaya. In this study, compositions of organic acids were assayed in different fruit developmental stages of ‘Guanhuabai’, ‘Guanhuahong’, ‘Wucihuanglong’, and ‘Youcihuanglong’ pitayas. Moreover, genes related to organic acid metabolism and subcellular localization of various HuIPMSs were analyzed. The present study provides insights of the key candidate genes involved in organic acid metabolism which can be used for fruit quality improvement in pitaya.

2. Materials and Methods

2.1. Plant Materials

In this study, four pitaya cultivars with different peel or pulp colors i.e., ‘Guanhuabai’ (‘GHB’, red peel with white pulp, *H. undatus*), ‘Guanhuahong’ (‘GHH’, red peel with red pulp, *H. monacanthus*), ‘Wucihuanglong’ (‘WCHL’, no thorns, yellow peel with white pulp, *H. undatus*), and ‘Youcihuanglong’ (‘YCHL’, thorns, yellow peel with white pulp, *H. megalanthus*) pitaya cultivars (Figure S1) were used as materials. Plants were cultivated in a commercial orchard from Madong Village, Baiyun District, Guangzhou City, Guangdong Province, China. In total, seven fruit developmental stages (S1–S7) of ‘GHH’ and ‘GHB’ (15, 17, 19, 23, 25, 27, and 32 days after artificial pollination, DAAP), ‘WCHL’ (14, 17, 19, 23, 25, 27, and 29 DAAP), and ‘YCHL’ (23, 35, 45, 55, 65, 70, and 75 DAAP) pitayas were collected with three biological repeats. Peels and pulps were separately collected and frozen in liquid nitrogen, then stored at -80°C until use.

In addition, *Nicotiana benthamiana* used for subcellular localization were cultivated in a greenroom at 23°C with a 16 h/8 h day/night photoperiod.

2.2. Determination of Organic Acids

Organic acids were extracted according to the method of Hu et al. [23]. Samples (400 mg) were dissolved in 10 mL 0.2% metaphosphoric acid (pre-cooled at 4°C) and disposed with ultrasonic concussion for 15 min, then centrifuged at $5000\times g$ at 4°C for 15 min. The supernatant (1 mL) was filtered through a $0.45\ \mu\text{m}$ microporous membrane, then transferred to an injection bottle for HPLC analysis using an Agilent HPLC series chromatograph equipped with a UV detector (Agilent Technologies, Palo Alto, CA, USA).

A Shim-packVP-ODSC18 column (5 μm particle size, 4.6 mm \times 150 mm) was used with a mobile phase of 0.2% metaphosphoric acid at a flow rate of 1.0 mL/min. The column temperature was 35 $^{\circ}\text{C}$, with an injection volume of 10 μL . Standard samples were produced with malic acid, citric acid, citramalic acid, oxalic acid, and ascorbic acid mixed with 0.2% metaphosphoric acid at gradient concentrations. The types and contents of organic acids were identified through a comparison of retention time and quantified by peak area.

2.3. RNA Extraction and cDNA Synthesis

Total RNA was extracted using the EASYspin Plus polysaccharide polyphenol complex plant RNA rapid extraction kit (RN53) (Aidlab, Beijing, China) according to the manufacturer's instructions. RNA integrity and concentration were checked by 1.0% agarose gel and a ScanDrop² nucleic acid detector (Analytik Jena, Jena, Germany), respectively. Qualified RNA was reverse-transcribed to cDNA using the *Evo M-MLV* RT Kit (AG11705) (Accurate Biology, Changsha, China).

2.4. Gene Expression Analyses

The RNA-Seq data (PRJNA704510) from four fruit developmental stages of 'GHH' and 'GHB' pitayas (S2, S4, S5 and S7) were used to draw the heatmap of transcript abundance by TBtools [24]. Specific primers (Table S1) were designed according to the selected sequence of pitaya organic acid metabolism-related enzyme genes using online software BatchPrimer3 v1.0 (<http://wheat.pw.usda.gov/demos/BatchPrimer3/>; accessed on 12 April 2019). The pitaya *Actin(1)* was used as the internal reference gene [25], and qRT-PCR analyses were performed on a CFX ConnectTM Real-Time PCR Detection System (Bio-Rad, Hercules, CA, USA) using SuperReal Color PreMix (SYBR Green) (FP215) (Tiangen Biotech, Beijing, China) with specific primers (Table S1). All experiments were repeated in triplicate. Gene expression was evaluated by the $2^{-\Delta\Delta\text{CT}}$ method [26].

2.5. Gene Isolation and Sequence Analyses

Based on the annotation files of pitaya genome and transcriptome databases, three candidate *IPMS* genes i.e., *HuIPMS1* (HU06G01828.1), *HuIPMS2* (HU08G00711.1), and *HuIPMS3* (HU01G02605.1), involved in citramalic acid synthase were obtained. The full length of *HuIPMS1*, *HuIPMS2*, and *HuIPMS3* were cloned from 'GHH' and 'GHB' cDNA using pEASY-Blunt Cloning Kits (TransGen Biotech, Beijing, China). DNAMAN 8 (Lynnon Biosoft, Pointe-Claire, QC, Canada) was used to design the amplification primers (Table S1). The basic physical and chemical properties of proteins were predicted using ProtParam (<https://web.expasy.org/protparam/>; accessed on 20 December 2019) and Pfam database (<https://pfam.xfam.org/>, accessed on 20 December 2019). Multiple alignments of deduced amino acid sequences were performed using DNAMAN8 software. Phylogenetic trees were constructed by MEGAX using the NJ (Neighbor-Joining) method with 1000 bootstrap replications.

2.6. Subcellular Localization

The PSORT online tool (<https://wolfpsort.hgc.jp>, accessed on 20 December 2019) was used to predict the subcellular localization of the *HuIPMS* proteins. The full-length cDNAs of *HuIPMS2* and *HuIPMS3* were cloned into pC18-35S::eGFP vector (Table S1), introduced into *Agrobacterium tumefaciens* strain GV3101 (pSoup-p19), and infiltrated into the leaves of *N. benthamiana* expressing a red fluorescent nuclear marker (Nucleus-RFP) or cell membrane marker (Membrane-RFP). Protoplasts were isolated from injected leaves of *N. benthamiana* plants after 2 d of cultivation in dark, and the fluorescence was observed by ZEISS LCM-800 confocal microscope (Carl Zeiss, Oberkochen, Germany).

2.7. Statistical Analysis

Statistical significance was determined by Duncan's multiple comparison tests at $p < 0.05$ or $p < 0.01$ using SPSS 26.0 (IBM, Chicago, IL, USA). Graphpad Prism 8.0 (GraphPad, Bethesda, MD, USA) was used for statistical analyses and plot graphs.

3. Results

3.1. Changes of Organic Acid Contents during Fruit Development of Pitayas

The organic acid contents were analyzed in pulps from seven fruit developmental stages of ‘GHH’, ‘GHB’, ‘WCHL’, and ‘YCHL’ pitayas (Figure 1). Malic acid contents in the pulps showed a trend of first rising and then falling during fruit development of the four pitaya cultivars (Table 1). In the white pulp cultivars, the malic acid content showed a slowly increasing trend in the early fruit developmental stage (S1–S3), while it decreased slightly in the red pulp cultivars.

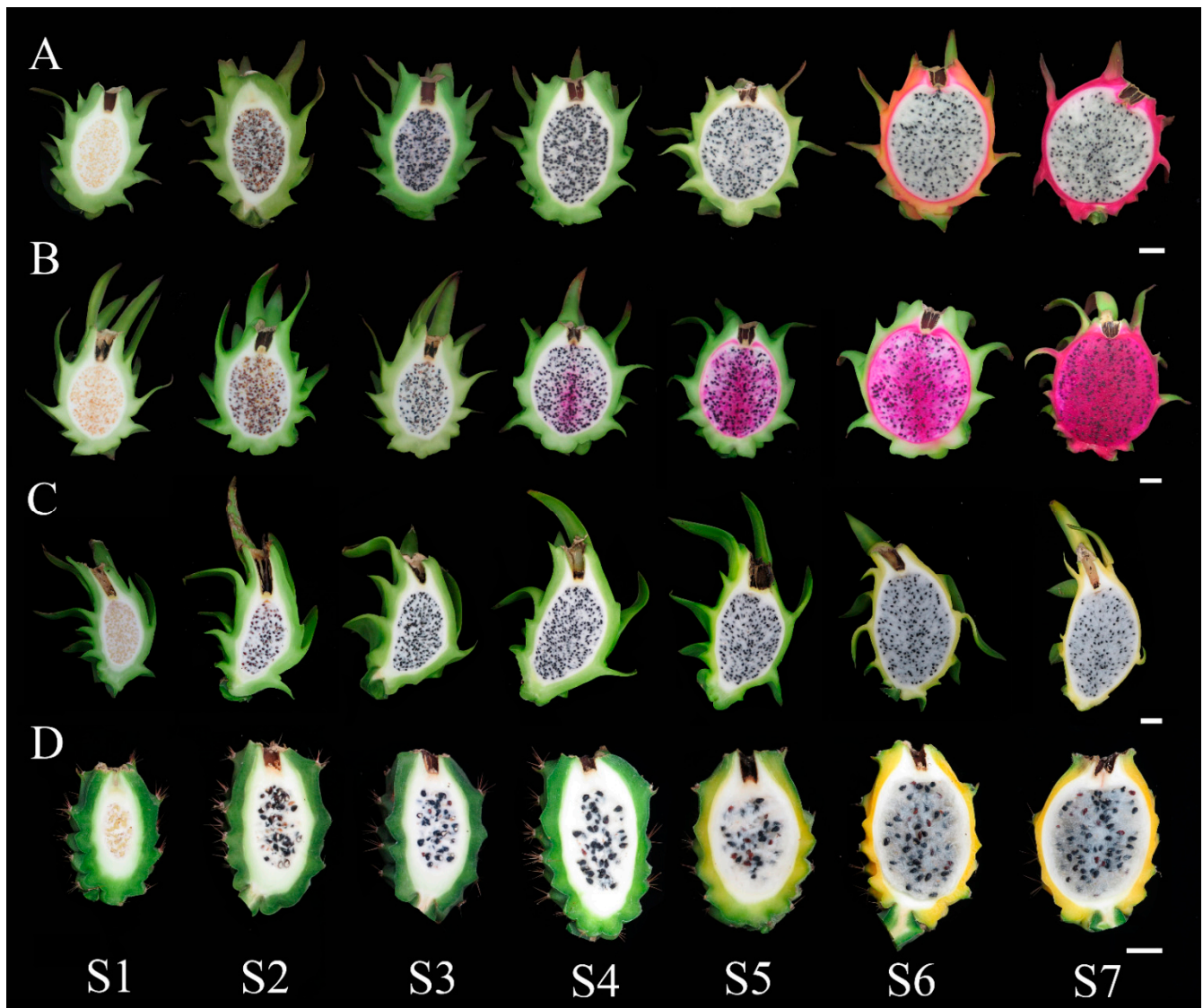


Figure 1. Pulp and peel coloration at different developmental stages of four pitaya cultivars. (A) ‘Guanhuabai’; (B) ‘Guanhuahong’; (C) ‘Wuchiuanglong’; (D) ‘Youcihuanglong’. Bars = 2 cm.

During fruit development, the citric acid contents in pulps of the ‘YCHL’ pitaya were significantly higher than that of ‘GHH’, ‘GHB’, and ‘WCHL’ pitayas. However, no citric acid was detected in pulps during the early fruit development stages of ‘GHB’ and ‘WCHL’ pitayas compared with ‘GHB’ and ‘WCHL’ pitayas, which peaked at S6 and S4 DAAP, respectively. With the exception of ‘GHB’ pitaya, citric acid was consistent with that of malic acid in ‘GHH’, ‘YCHL’, and ‘WCHL’ pitayas, which was possibly correlated (Table 1).

Table 1. Compositions of organic acids in four different pitaya cultivars.

| Cultivars (<i>n</i> = 3) | Stages | Contents (mg/g) | | | | |
|---------------------------|--------|------------------|------------------|-------------------|------------------|------------------|
| | | Malic Acid | Citric Acid | Citramalic Acid | Oxalic Acid | Ascorbic Acid |
| 'GHH' | S1 | 2.177 ± 0.064 d | 0.481 ± 0.018 b | 3.136 ± 0.609 bc | 0.515 ± 0.077 b | 0.123 ± 0.004 a |
| | S2 | 1.753 ± 0.326 d | 0.377 ± 0.063 b | 3.997 ± 0.309 ab | 0.713 ± 0.087 a | 0.105 ± 0.015 bc |
| | S3 | 1.638 ± 0.460 d | 0.385 ± 0.106 b | 3.542 ± 0.856 abc | 0.514 ± 0.040 b | 0.067 ± 0.024 b |
| | S4 | 5.487 ± 0.984 c | 0.543 ± 0.100 b | 4.380 ± 0.306 a | 0.434 ± 0.036 bc | 0.065 ± 0.021 b |
| | S5 | 11.133 ± 0.729 b | 0.849 ± 0.13 ab | 3.662 ± 0.28 abc | 0.451 ± 0.131 bc | 0.066 ± 0.018 b |
| | S6 | 13.493 ± 1.430 a | 1.218 ± 0.375 a | 2.609 ± 0.192 c | 0.413 ± 0.040 bc | 0.066 ± 0.007 b |
| | S7 | 7.228 ± 0.523 c | 1.055 ± 0.090 a | 0.209 ± 0.061 d | 0.283 ± 0.056 c | 0.022 ± 0.011 c |
| 'GHB' | S1 | 2.922 ± 0.247 d | 0.000 ± 0.000 b | 4.062 ± 0.699 b | 0.054 ± 0.018 c | 0.179 ± 0.016 a |
| | S2 | 3.990 ± 0.646 cd | 0.000 ± 0.000 b | 5.597 ± 0.000 a | 0.095 ± 0.021 b | 0.203 ± 0.013 a |
| | S3 | 4.449 ± 0.062 cd | 0.000 ± 0.000 b | 5.931 ± 0.880 a | 0.139 ± 0.009 a | 0.178 ± 0.030 a |
| | S4 | 15.196 ± 1.500 a | 0.165 ± 0.030 a | 4.295 ± 0.187 b | 0.073 ± 0.024 bc | 0.090 ± 0.006 b |
| | S5 | 18.116 ± 2.735 a | 0.122 ± 0.030 a | 3.160 ± 0.228 bc | 0.072 ± 0.014 bc | 0.048 ± 0.006 c |
| | S6 | 7.159 ± 0.204 c | 0.202 ± 0.023 a | 2.693 ± 0.283 c | 0.036 ± 0.011 c | 0.034 ± 0.002 c |
| | S7 | 11.072 ± 1.226 b | 0.138 ± 0.018 a | 1.241 ± 0.071 d | 0.041 ± 0.003 c | 0.052 ± 0.003 c |
| 'WCHL' | S1 | 0.848 ± 0.0140 e | 0.000 ± 0.000 d | 4.045 ± 0.059 b | 0.582 ± 0.012 a | 0.280 ± 0.007 a |
| | S2 | 1.489 ± 0.152 e | 0.000 ± 0.000 d | 4.499 ± 0.406 b | 0.526 ± 0.155 a | 0.185 ± 0.034 b |
| | S3 | 3.379 ± 1.076 d | 0.433 ± 0.210 c | 5.815 ± 0.310 a | 0.323 ± 0.067 b | 0.154 ± 0.003 b |
| | S4 | 13.997 ± 1.095 a | 1.704 ± 0.219 a | 4.021 ± 0.205 b | 0.256 ± 0.071 bc | 0.185 ± 0.004 b |
| | S5 | 10.183 ± 0.507 b | 0.952 ± 0.083 b | 1.437 ± 0.078 c | 0.248 ± 0.067 bc | 0.093 ± 0.003 c |
| | S6 | 5.624 ± 0.313 c | 0.451 ± 0.018 c | 0.910 ± 0.000 d | 0.154 ± 0.033 c | 0.058 ± 0.001 d |
| | S7 | 5.945 ± 0.950 c | 0.569 ± 0.110 c | 0.293 ± 0.010 e | 0.189 ± 0.029 bc | 0.047 ± 0.009 d |
| 'YCHL' | S1 | 2.422 ± 0.140 de | 1.818 ± 0.237 f | 1.561 ± 0.237 b | 0.692 ± 0.022 a | 0.220 ± 0.012 a |
| | S2 | 2.698 ± 0.140 cd | 2.503 ± 0.135 e | 1.935 ± 0.260 a | 0.653 ± 0.021 a | 0.177 ± 0.015 a |
| | S3 | 3.058 ± 0.071 c | 3.060 ± 0.126 de | 1.498 ± 0.092 b | 0.690 ± 0.005 a | 0.196 ± 0.014 a |
| | S4 | 5.122 ± 0.275 a | 6.736 ± 0.418 a | 0.632 ± 0.054 c | 0.617 ± 0.036 a | 0.120 ± 0.039 b |
| | S5 | 3.837 ± 0.400 b | 5.125 ± 0.224 b | 0.000 ± 0.000 d | 0.458 ± 0.003 b | 0.006 ± 0.001 c |
| | S6 | 2.138 ± 0.162 e | 4.185 ± 0.261 c | 0.000 ± 0.000 d | 0.331 ± 0.040 c | 0.003 ± 0.000 c |
| | S7 | 1.576 ± 0.202 f | 3.620 ± 0.298 cd | 0.000 ± 0.000 d | 0.263 ± 0.075 c | 0.015 ± 0.001 c |

Each sample is repeated three times. The different lowercase letters following the numbers indicate a significant difference ($p < 0.05$) between the cultivars.

Contents of citramalic acid showed an upward trend in the early stage of fruit development of the four cultivars. The highest contents of citramalic acid i.e., 5.93 mg/g and 5.82 mg/g were detected at S3 in 'GHB' and 'WCHL' pitayas, respectively, and declined thereafter. Citramalic acid in the 'GHH' pitaya reached its maximum (4.38 mg/g) at S4. Compared with 'GHH', 'GHB', and 'WCHL' pitayas, lower contents of citramalic acid were detected throughout the fruit development of the 'YCHL' pitaya. The highest content of citramalic acid (1.94 mg/g) was obtained at S2 of the 'YCHL' pitaya, and then gradually declined thereafter until disappeared after S5 (Table 1).

'GHH', 'GHB', 'YCHL', and 'WCHL' pitayas had relatively high levels of oxalic acid at early fruit development, and gradually decreased during fruit maturation. Ascorbic acid showed a downward trend during the fruit development of the four pitaya cultivars (Table 1).

3.2. Changes of Total Organic and Composition Ratios

During the fruit development of the four pitaya cultivars, the total organic acid content in the pulp showed a trend of first rising and then falling, which was similar to that of malic acid. During the first three developmental stages (S1–S3) of 'GHB', 'GHH', and 'WCHL' pitayas, the predominant organic acid was citramalic acid, followed by malic acid. During the mature stage of 'GHB', 'GHH', and 'WCHL' pitayas, the main organic acid was malic acid (accounting for 88.64%, 82.36% and 89.63% of the total acid), followed by citramalic acid (9.93%), citric acid (12.03%), and citric acid (6.83%), respectively (Table 1). Regarding the 'YCHL' pitaya, malic acid (37.30%), citric acid (28.00%), and citramalic acid (24.04%) were mainly accumulated at the early stage. The

highest content of total organic acids (13.11 mg/g) was detected at S4, and decreased thereafter. Citric acid was the main organic acid during fruit development. During the mature stage, the main organic acids were citric acid (64.67%) and malic acid (28.75%). In the mature fruit, the order of the total organic acid content from high to low was: ‘GHB’ > ‘GHH’ > ‘WCHL’ > ‘YCHL’ (Table 1).

3.3. Analyses of Transcriptome Data of ‘GHB’ and ‘GHH’ Pitayas

Overall, eight transcriptome databases, from GHH17, GHH23, GHH25, and GHH32 (‘Guanhuahong’ at S2, S4, S5, and S7) and GHB17, GHB23, GHB25, and GHB32 (‘Guanhuabai’ at S2, S4, S5, and S7) were constructed. In total, 99.32%, 99.27%, 99.02%, 99.66%, 98.87%, 99.72%, 99.51%, and 99.80% clean reads were respectively achieved after filtering out low-quality, contaminated joints and high unknown bases (Table S2).

In the pitaya transcriptome data, $\text{padj} < 0.05$ was used as the standard to screen differentially expressed genes (DEGs). The comparison between GHB23 vs. GHB17 and GHH23 vs. GHH17 resulted in a total of 581 DEGs (299 up-regulated genes and 282 down-regulated genes), and 1131 DEGs (713 up-regulated genes and 418 down-regulated genes), respectively (Figure S2A,B). Only 75 DEGs (38 up-regulated genes and 37 down-regulated genes) were detected in GHB25 vs. GHB23, while 1256 DEGs (953 up-regulated genes and 303 down-regulated genes) were found in GHH25 vs. GHH23 (Figure S2C,D). A total of 2427 and 1386 genes were differentially expressed in the GHB32 vs. GHB25 and GHH32 vs. GHH25, respectively, among which 941/358 genes were up-regulated, and 1486/1028 genes were down-regulated (Figure S2E,F).

To further study those DEGs involved in biological pathways, the Kyoto Gene and Genome Encyclopedia (KEGG) database was used for DEG classification. The 20 top-ranked pathways were listed in Figure 2. In comparisons of GHH17 vs. GHB17, GHH23 vs. GHB23, GHH25 vs. GHB25, and GHH32 vs. GHB32, the highest number of enriched DEGs referred to metabolic pathways and biosynthesis of secondary metabolites. Pyruvate metabolism and carbon metabolism including synthesis of acetyl-CoA, malic acid, and citric acid were found, indicating differences in organic acid metabolism between ‘GHH’ and ‘GHB’ pitaya fruit at different stages.

3.4. Expression Analyses of Organic Acid Metabolism-Related Genes

To explore the mechanism of organic acid accumulation in pitaya, 14 *citrate synthase* (CS) genes, eight *isocitrate dehydrogenase* (IDH) genes, six *aconitase* (ACO) genes, 40 *malate dehydrogenase* (MDH) genes, 11 *malic enzymes* (ME) genes, 24 *phosphoenolpyruvate carboxykinase* (PEPC) genes, one *malate synthase* (MS) gene, and three *2-isopropylmalate synthase* (IPMS) genes were identified based on the functional annotations of the pitaya genome and transcriptome database. A heatmap was drawn according to the FPKM value of the corresponding gene in the transcriptome database at different fruit developmental stages (Figure 3).

After removal of low expressed genes in the ‘GHB’ and ‘GHH’ pitaya transcriptome database, nine CSs, five ACOs, three *NAD-IDHs*, three *NADP-IDHs*, seven *NAD-MDHs*, six *NADP-MDHs*, five *NAD-MEs*, six *NADP-MEs*, seven *PEPCs*, one *MS*, and three *IPMSs* were selected for further analyses. The citric acid content in the ‘GHH’ pulp was significantly negatively correlated with *NADP-IDH3* gene expression, while malic acid content was significantly negatively correlated with *NADP-ME5* and *PEPC3* expression during fruit maturation. In the ‘GHB’ pitaya, the changes of *NADP-MDH6* and *PEPC4* were significantly positively correlated with malic acid, while *MS* positively correlated with citric acid. In the ‘YCHL’ pitaya, *NAD-MDH2* and *MS* demonstrated significant positive correlation with malic acid, and the expression of *NADP-MDH6* in the ‘WCHL’ pitaya also showed a positive correlation. However, no significant correlation was found for *NAD-MDHs*, *NADP-MDHs*, *MS*, *PEPCs*, and *NAD-MEs* (Figure 4, Tables S3 and S4).

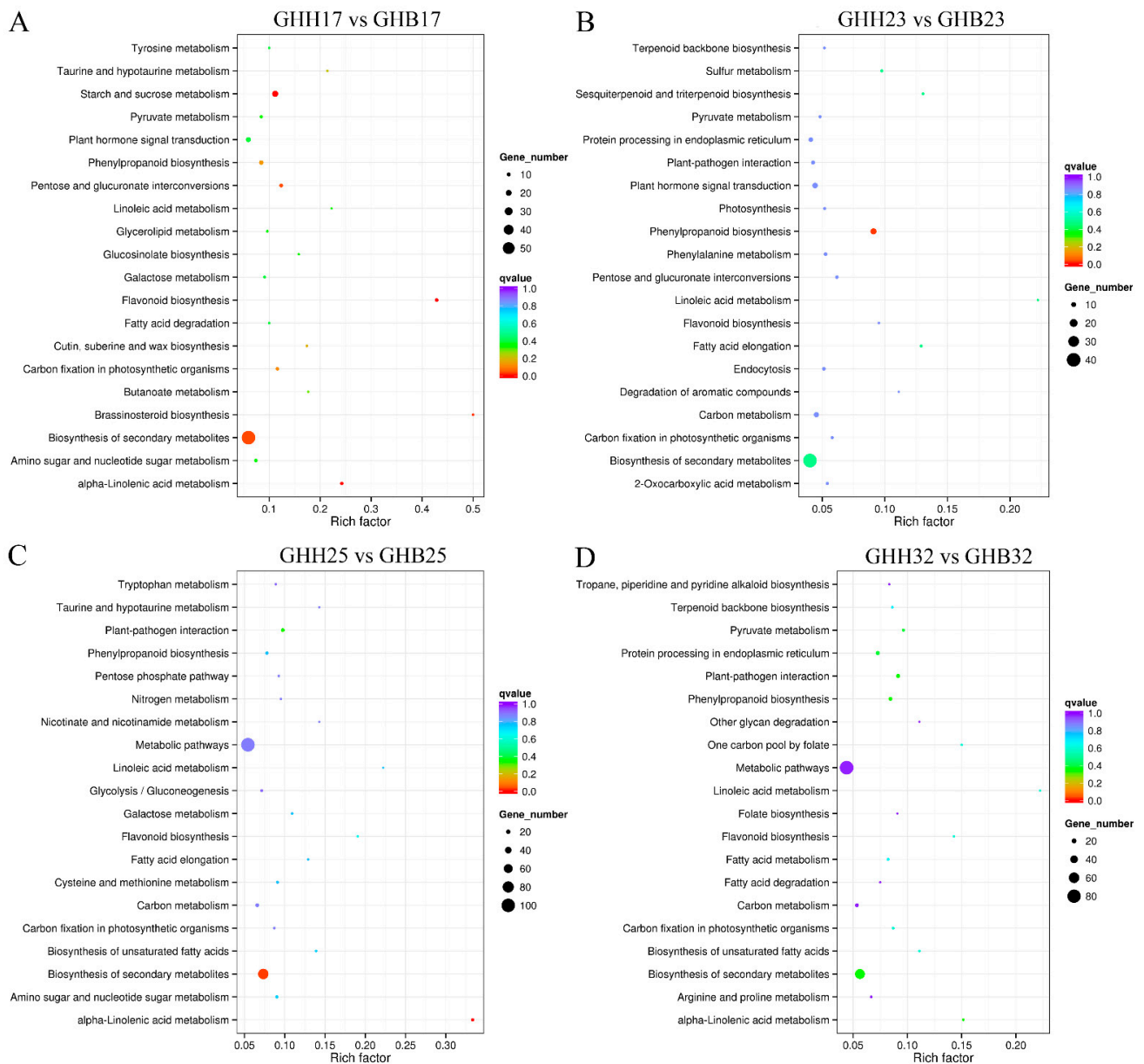


Figure 2. KEGG enrichment of DEGs in (A) GHH17 vs. GHB17, (B) GHH23 vs. GHB23, (C) GHH25 vs. GHB25, and (D) GHH32 vs. GHB32. The X axis is the Rich Ratio (Rich Ratio is calculated as candidate gene number in a specific term/total gene numbers), and the Y axis represents KEGG pathway. The size of the bubble indicates the number of genes annotated to KEGG pathway. The color represents the enriched Q-value ranges from red (low value) to blue (high value).

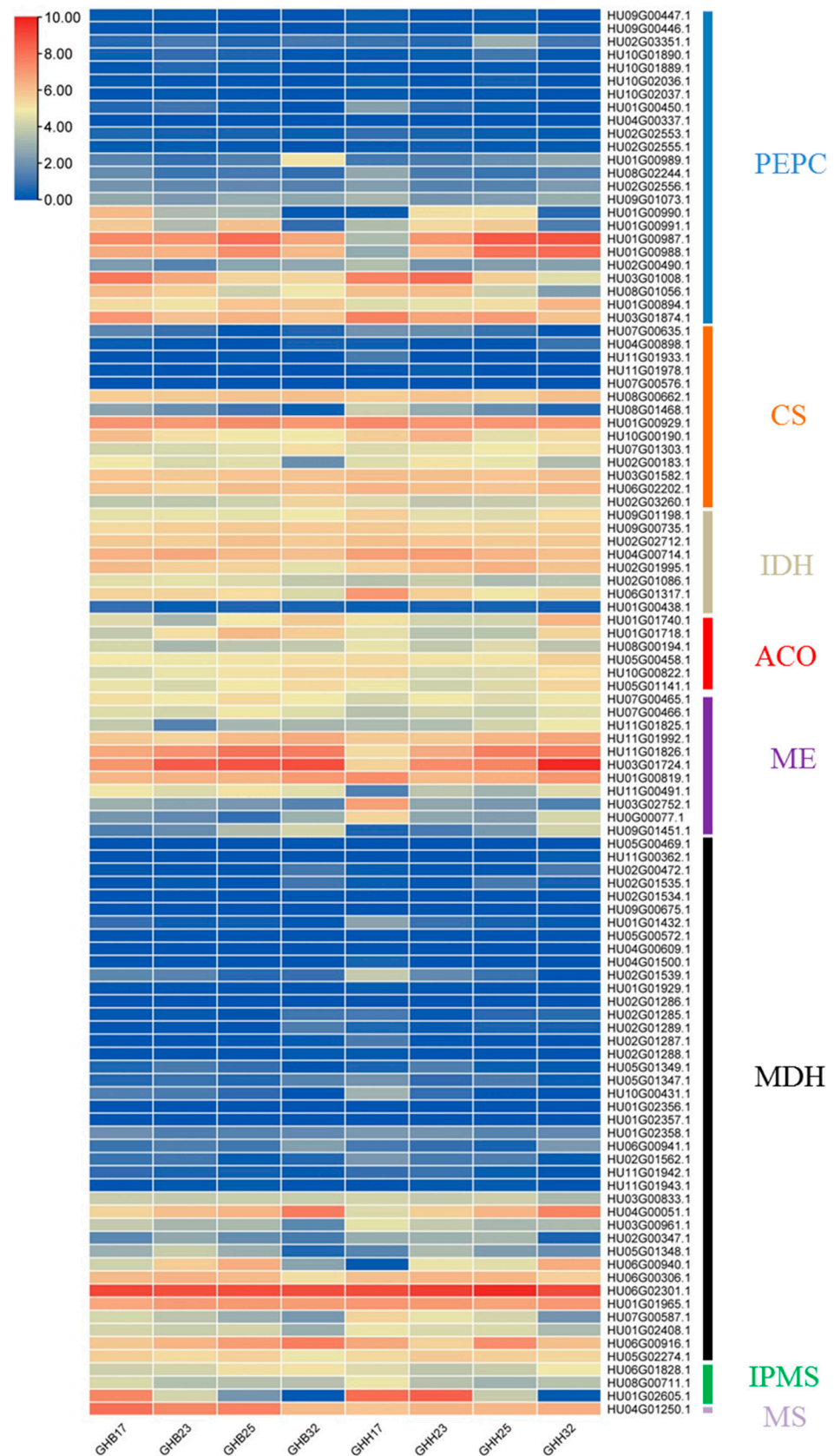


Figure 3. The expression heatmap of genes related to organic acid metabolism according to the RNA-Seq datasets of ‘GHB’ and ‘GHH’ pitaya pulps. The color bar represents the log₂ (FPKM) and ranges from blue (low expression) to red (high expression).

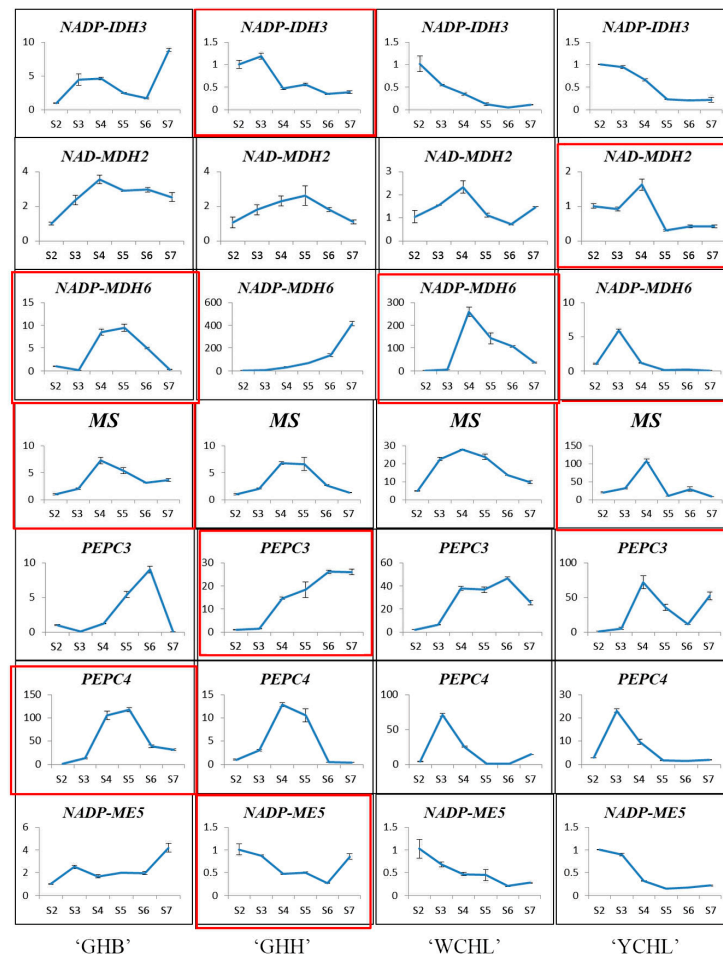


Figure 4. Expression analyses of genes related to organic acid metabolism at different fruit developmental stages of four pitaya cultivars by qRT-PCR. The X axis represents six fruit developmental stages of four pitaya cultivars. The Y axis represents relative expression level. The red boxes represent expression level of genes significantly associated with citric or malic acid contents. All data are normalized by Actin(1).

3.5. Cloning, Sequence and Evolutionary Analyses of HuIPMS

To explore the functions of *HuIPMS1*, *HuIPMS2*, and *HuIPMS3* in citramalic acid synthesis in pitaya, their full-length cDNAs were cloned. The complete open reading frames (ORFs) of *HuIPMS1*, *HuIPMS2*, and *HuIPMS3* were 1911 bp, 1911 bp, and 921 bp, respectively, and the amino acid sequences encoded by these three genes were identical to each other in the transcriptome databases of 'GHB' and 'GHH' pitayas. *HuIPMS1* had 82.34% sequence identity to *HuIPMS2*, but only 26.53% to *HuIPMS3*, and *HuIPMS2* showed 27% identity to *HuIPMS3*. *HuIPMS1* and *HuIPMS2* both encoded a protein composed of 636 amino acids with molecular weights of 68.57 kDa and 68.42 kDa, and pIs of 6.43 and 7.25, respectively. *HuIPMS3* encoded a protein containing 306 amino acids with a molecular weight of 33.95 kDa and a pI of 6.47. The instability indexes of *HuIPMS1*, *HuIPMS2*, and *HuIPMS3* were respectively 35.25, 39.04, and 24.59, and classified as stable proteins (Less than 40). The average hydropathicity for *HuIPMS1*, *HuIPMS2*, and *HuIPMS3* were respectively -0.141 , -0.159 , and -0.274 , which shows a hydrophilic nature (less than 0) (Table S5).

HuIPMS1 and *HuIPMS2* both contained HMGL-like and LeuA_dimer domains, while *HuIPMS3* only contained an HMGL-like domain (Figure S2). Moreover, the phylogenetic tree of IPMS proteins showed that *HuIPMS1* and *HuIPMS2* shared a closer phylogenetic relationship with IPMSs from *Beta vulgaris*, *Chenopodium quinoa*, and *Spinacia oleracea*, while *HuIPMS3* was closely related to *Malus Domestica* (Figure S3).

3.6. Expression Analyses of *HuIPMSs*

The expression patterns of *HuIPMSs* were analyzed at different fruit development stages of ‘GHH’, ‘GHB’, ‘YCHL’, and ‘WCHL’ pitayas. *HuIPMS1* was irregularly expressed in the four pitaya cultivars, and the correlation between expression level of *HuIPMSs* and the citramalic acid content at different fruit development stages showed similar changing patterns (Figure 5A). The relative expression level of *HuIPMS2* generally increased first, and then decreased in the three white pulp cultivars i.e., ‘GHB’, ‘YCHL’, and ‘WCHL’ pitayas, which was positively related to the changing trend of citramalic acid in the red pulp cultivar ‘GHH’ pitaya (Figure 5B). During fruit development of the four pitaya cultivars, *HuIPMS3* showed a trend of high expression during the early stages, and extremely low at later stages. Among them, the relative expression level of ‘YCHL’ at S1 was significantly higher than the other stages (Figure 5C).

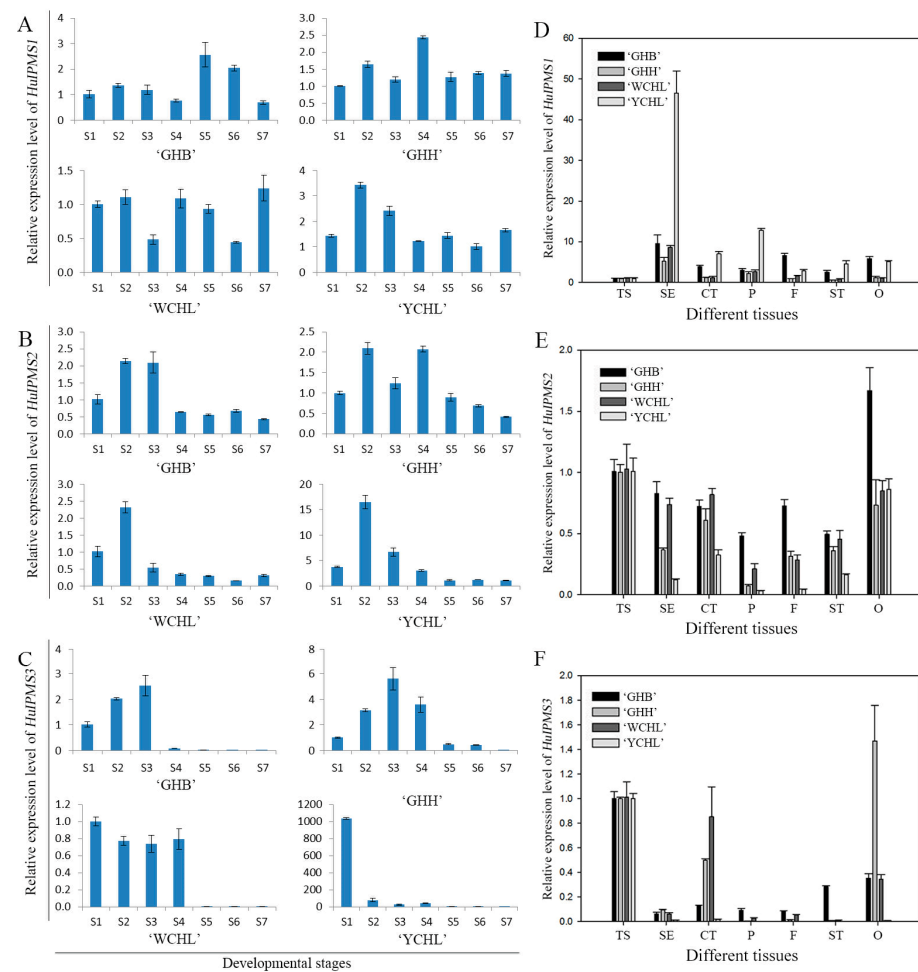


Figure 5. Expression analyses of *HuIPMSs* by qRT-PCR. The expression of *HuIPMS1* (A), *HuIPMS2* (B), and *HuIPMS3* (C) in fruit development of four pitaya cultivars, and *HuIPMS1* (D), *HuIPMS2* (E), *HuIPMS3* (F) in different pitaya tissues. The X axis for (A–C) represents seven fruit developmental stages of four pitaya cultivars. The X axis for (D–F) represent different pitaya tissues. TS, Tender stem; SE, Sepal; CT, Calyx tube; P, Petal; F, Filament; ST, Style; O, Ovary. All data are normalized by Actin1(1).

The expression levels of *HuIPMS1*, *HuIPMS2* and *HuIPMS3* were analyzed in various tissues of ‘GHH’, ‘GHB’, ‘YCHL’, and ‘WCHL’ pitayas. *HuIPMS1* was predominantly expressed in the sepals of the four pitaya cultivars, the petals of ‘YCHL’, and the filaments and ovaries of the ‘GHB’ pitaya (Figure 5D). The highest expression level of *HuIPMS2* was detected in the ovaries of the ‘GHB’ pitaya, followed by the tender stems and calyx tubes (Figure 5E). *HuIPMS3* showed high expression levels in the tender stems of four pitaya

cultivars, compared with the highest expression level in the ovaries of the ‘GHH’ pitaya (Figure 5F).

Pearson’s correlation test was used to analyze the correlation between citramalic acid contents and *HuIPMSs* gene expression in the four pitaya cultivars. No significant correlation was found between citramalic acid contents and *HuIPMS1*. The expression level of *HuIPMS2* was positively correlated with the four pitaya cultivars with correlation coefficients of 0.871, 0.786, 0.473, and 0.811, respectively. A similar correlation was detected between citramalic acid contents and *HuIPMS3* with the correlation coefficients of 0.848, 0.590, 0.886, and 0.453, respectively (Table 2).

Table 2. Correlation analysis between citramalic acid contents and expression levels of *HuIPMSs*.

| Cultivars | <i>HuIPMS1</i> | <i>HuIPMS2</i> | <i>HuIPMS3</i> |
|-----------|----------------|----------------|----------------|
| ‘GHB’ | −0.083 | 0.871 * | 0.848 * |
| ‘GHH’ | 0.350 | 0.786 * | 0.590 |
| ‘WCHL’ | −0.072 | 0.473 | 0.886 ** |
| ‘YCHL’ | 0.782 | 0.811 * | 0.453 |

* and ** represent significantly difference at $p < 0.05$ and $p < 0.01$, respectively.

3.7. Subcellular Localization of *HuIPMSs* Protein

The PSORT online tool was used to predict the subcellular localization of *HuIPMSs* protein. *HuIPMS2* was located in the chloroplast, while *HuIPMS3* was located in the cytoplasm and mitochondria. To further verify the subcellular localization of *HuIPMS2* and *HuIPMS3* in pitaya, transient expression vectors of 35S-IPMS2-GFP and 35S-IPMS3-GFP were constructed and transiently expressed in *N. benthamiana* leaves. The results showed that *HuIPMS2* was localized in the chloroplast, while *HuIPMS3* appeared to be localized in the cell membrane, cytoplasm, and nucleus (Figure 6A).

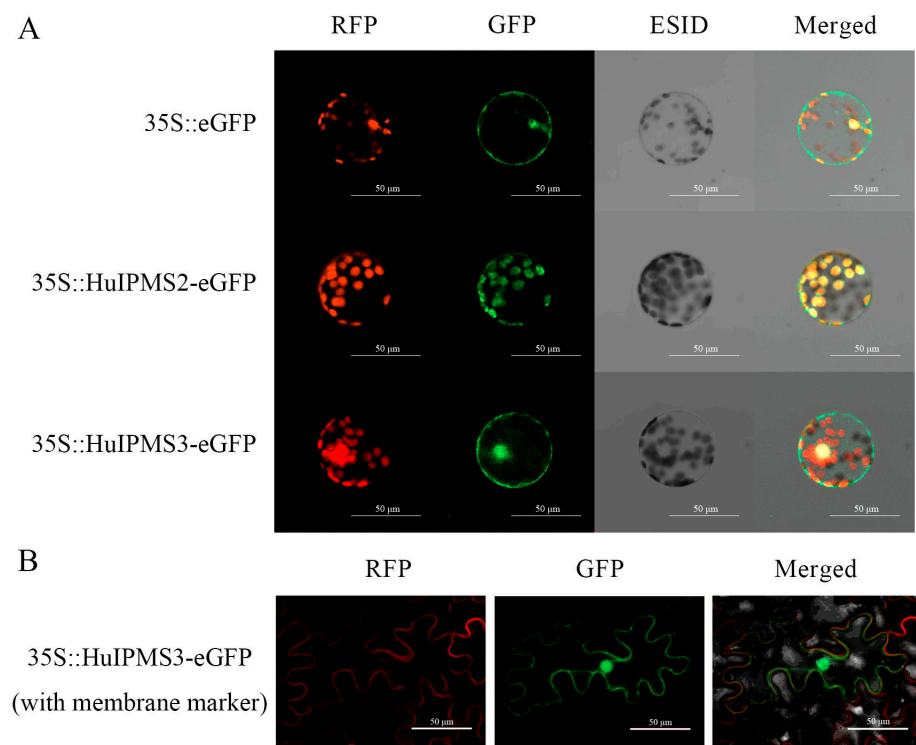


Figure 6. Subcellular location analyses of (A) *HuIPMS2* and *HuIPMS3* in the protoplasts, and (B) *HuIPMS3* in the leaves of *N. benthamiana*. Green and red signals represent green fluorescent protein and red fluorescent protein, respectively. ESID, bright field. Scale bars = 50 μm.

To further determine the localization of *HuIPMS3*, 35S-IPMS3-GFP was transiently expressed in the leaves of *N. benthamiana*, expressing a red fluorescent membrane marker. The results indicated that *HuIPMS3* presented a cytoplasmic-like and nuclear subcellular localization (Figure 6B).

4. Discussion

4.1. Accumulation of Organic Acids in the Four Pitaya Cultivars

Organic acids in fruits are generally divided into two types: citric acid- and malic acid-accumulated patterns [3]. In this study, 'GHB', 'GHH', and 'WCHL' pitayas mainly accumulated malic acid during the mature stage (S6–S7), which was consistent with previous studies [21,22], whereas the 'YCHL' pitaya mainly accumulated citric acid in mature fruits (Table 1). The type and content of organic acids and the sugar/acid ratio are the important basis for the form of fruit flavor. Sugars affect the degree of sweetness, while organic acids are responsible for the sour taste [27]. In terms of flavor, the taste of the 'WCHL' pitaya was better and sweeter, consistent with its lowest total acid content in mature fruit pulp among the four pitaya cultivars. During the fruit development of many types of fruits, the content of organic acids shows an increase during the early stages, and gradually decreases as the fruit matures [28–30]. At different stages of fruit development, significant differences in the types and ratios of organic acids can be detected. For example, the contents of chlorogenic acid and ascorbic acid are significantly higher in semi-matured mulberry fruits (*Morus alba* Linnaeus) [31]. Kiwifruit (*Actinidia chinensis*) is rich in quinic acid in the young fruit stage, and gradually proceeded to malic acid- and citric acid-dominant phase as fruit matures [32]. Citramalic acid content reached its maximum during the fruit coloring-onset stage of the pitaya (*H. polyrhizus* cv. Zihonglong) suggesting that it was associated with betalain synthesis [22]. In this study, citramalic acid was the main organic acid during the early fruit stages (S1–S3) of 'WCHL', 'GHH', and 'GHB' pitayas, and decreased gradually thereafter, finally dominated by malic acid or citric acid at a more mature stage (Table 1). The highest contents of citramalic acid were observed during the early fruit developmental stage (S3) to the pulp coloring-onset stage (S4), which is consistent with previous findings in the pitaya fruit [22]. In fruit cells, pyruvate is catalyzed by the pyruvate dehydrogenase complex to produce acetyl-CoA, and citrate synthase (CS) catalyzes the synthesis of citric acid from acetyl-CoA and oxaloacetate. Therefore, there may be a competition relationship between IPMS and CS for the same reaction substrate [33]. Moreover, pyruvate is another substrate for the synthesis of citramalic acid, which can be obtained from the degradation of malic acid. In this study, citramalic acid mainly accumulated during the early fruit developmental stage of the four pitaya cultivars. However, levels of citric acid and malic acid content were lower at these stages. These results indicated that citramalic acid may affect the accumulation of citric acid and malic acid in pitayas, thus involved in improving the flavor. (Table 1).

4.2. The Relationship between Organic Acid Contents and Metabolism-Associated Genes

PEPC mainly catalyzes phosphoenolpyruvate (PEP) to generate oxaloacetate (OAA) and inorganic phosphorus, and PEPC regulates its activity through phosphorylation-dephosphorylation [34]. PEPC can regulate the malic acid content during fruit development of loquat (*Eriobotrya japonica*) [3]. In this study, *PEPC4* and *MS* in the 'GHB' pitaya, and *PEPC3* in the 'GHH' pitaya were significantly positively correlated with the content of malic acid (Figure 4 and Table S3). Moreover, a positive correlation was observed between malic acid and *MS* and *NAD-MDH2* in the 'YCHL' pitaya. These results suggested that *PEPC4*, *MS*, and *NAD-MDH2* may be involved in the positive regulation of malic acid metabolism. *MDH* mainly catalyzes the formation of malic acid from OAA in the TCA cycle of fruits, which is the most likely route of malate formation [35]. In apples, the *MdcyMDH* gene mainly plays a role in the synthesis of malic acid [36]. In the present study, the expression levels of *NADP-MDH6* were significantly positively correlated with the dynamic trend of malic acid content during the fruit development of 'GHB' and 'WCHL' pitayas, indicating

that *NADP-MDH6* positively regulated the accumulation of malic acid in the two pitaya cultivars. Afterward, *NADP-ME* catalyzes a reversible oxidative decarboxylation of malic acid to produce pyruvate [37]. The expression level of *NADP-ME* decreased in the ‘Huang guan’ pear (*Pyrus pyrifolia* Nakai) which was treated with CaCl_2 , accompanied by weakness of malic acid degradation [38]. A similar expression pattern of *NADP-ME5* was found in pitaya, suggesting that *NADP-ME5* could promote the *NADP-ME* synthesis involving malic acid degradation.

CS directly controls citric acid synthesis [39]. However, no significant correlation was found between the *CS* gene expression and the citric acid contents during the different fruit developmental stages of the four pitaya cultivars (Figure 4 and Table S4), which was different from the recently published results of citric acid in passion fruits [40].

4.3. Role of *HuIPMS2* in Citramalic Acid Synthesis of Pitaya

Citramalate synthase belongs to the 2-isopropylmalate synthase family [41]. Genes in this family have a conserved C-terminal $(\beta\beta\beta\alpha)_2$ LeuA dimer domain connected by a flexible linker region. Moreover, their 3D structures and catalytic mechanism are similar [8]. Enzymes related to the catalytic domain of the N-terminal TIM barrel (Pfam ID: PF00682) include 2-isopropylmalate synthase, citramalate synthase, homocitrate synthase, pyruvate carboxylase, 4-hydroxy-2-oxvalerate aldolase and hydroxymethylglutaryl-CoA lyase, while the activity of the enzymes containing the C-terminal LeuA dimer domain is limited to 2-isopropylmalate synthase and citramalate synthase only, which catalyzes the first step of the biosynthesis of L-leucine and L-isoleucine, respectively [8]. In this study, three *IPMS* genes were identified according to structural domain annotation in the pitaya genome and transcriptome database. Both *HuIPMS1* and *HuIPMS2* contained HMGL-like and LeuA_dimer domains (Figure S3B), the same as *MJ1392* [10], whose corresponding function of catalyzing the synthesis of citramalic acid has been verified by transforming into *E. coli* [13,42,43]. *HuIPMS3* only contained the HMGL-like domain. *HuIPMS1* was preferentially expressed in the sepals, while the highest expression levels of *HuIPMS2* and *HuIPMS3* were detected in tender stems and ovaries, indicating that *HuIPMSs* genes have different expression patterns in various pitaya tissues and organs (Figure 5D–F). In the four cultivars of pitaya, the changing tendency of *HuIPMS2* expression level was significantly positively correlated with the dynamic changes of citramalic acid content (Table 2). *HuIPMS2* protein localized to chloroplasts, while *HuIPMS3* protein appeared to have accumulated in the cytoplasm and nucleus (Figure 6). Recently, the *IPMS* gene *MdCMS*, previously only described in microorganisms, was first cloned and verified to participate in citramalic pathway in apple [7]. In *Arabidopsis thaliana*, the *AtMAM3* protein has been proven that can condense various 2-oxo acids with an acyl-CoA ester [44]. A common gene family, conserved domains, and subcellular localization among *HuIPMS2*, *AtMAM3* and *MdCMS* proteins may predict their functional consistency.

5. Conclusions

In this study, organic acid compositions and contents, as well as expression patterns of key genes related to organic acid metabolism were analyzed during fruit maturation of ‘Guanhuabai’ (GHB), ‘Guanhuahong’ (GHH), ‘Wucihuanglong’ (WCHL), and ‘Youcihuanglong’ (YCHL) pitayas. ‘GHB’, ‘GHH’, and ‘WCHL’ were malic acid-accumulating fruits, while ‘YCHL’ was citric acid-accumulating fruit. The highest content of citramalic acid was detected from the early fruit developmental stage (S3) to the coloring-onset stage (S4). *PEPC4*, *MS*, and *NADP-MDH6* are the key genes involved in regulating malic acid metabolism in the ‘GHB’ pitaya, while *NADP-ME5*, and *PEPC3* are important in the ‘GHH’ pitaya. The *NADP-MDH6* gene plays a major role in malic acid synthesis in the ‘WCHL’ pitaya. *MS* and *NAD-MDH2* are involved in the regulation of malic acid in the ‘YCHL’ pitaya. *HuIPMSs* had obvious expression differences in different tissues and organs, of which *HuIPMS1* had highest expression level in sepals, compared with highest expression levels of *HuIPMS2* and *HuIPMS3* in tender stems and ovaries. *HuIPMS2* was located in the

chloroplast with HMGL-like and LeuA_dimer conserved domains. The relative expression of *HuIPMS2* gene was positively correlated with the content of citramalic acid.

Supplementary Materials: The following supporting information can be downloaded at: <https://www.mdpi.com/article/10.3390/horticulturae8020167/s1>, Figure S1: Four different peel and pulp pitaya cultivars used in this study, Figure S2: Comparison of gene regulation at different fruit stages in ‘GHB’ and ‘GHH’ pitayas, Figure S3: Cloning, sequence and evolutionary analyses of *HuIPMSs*, Table S1: Table S1 Primers used for RT-qPCR and gene cloning, Table S2: Statistical analyses of transcriptome data, Table S3: Correlation analyses between malic acid contents and expression levels of related-genes, Table S4: Correlation analyses between citric acid contents and expression levels of related-genes, Table S5: Physical and chemical properties of *HuIPMS1*, *HuIPMS2* and *HuIPMS3*.

Author Contributions: Conceptualization, Y.Q.; Methodology and validation, J.C. (Jiaxuan Chen) and Y.Y.; Formal analysis, investigation, resources, data curation and visualization, J.C. (Jiaxuan Chen), Y.Y., F.X., J.C. (Jianye Chen), Z.Z., R.Z., J.Z. and G.H.; Writing—original draft preparation, J.C. (Jiaxuan Chen) and Y.Y.; Supervision, Y.Q.; Project administration, G.H. and Y.Q.; Funding acquisition, J.C. (Jianye Chen), G.H. and Y.Q. All authors have read and agreed to the published version of the manuscript.

Funding: This research was funded by the Key Science and Technology Planning Project of Guangzhou (grant no. 201904020015), Science and Technology Program of Guangzhou (grant no. 202002020060) and Zhanjiang (grant no. 2019A01003).

Institutional Review Board Statement: Not applicable.

Informed Consent Statement: Not applicable.

Data Availability Statement: Data is contained within the article. Accession Numbers: Sequence data from this article can be found in the pitaya genome (<http://www.pitayagenomic.com/>, accessed on 20 December 2019) or NCBI GenBank databases under the following accession numbers: *HuIPMS1*, OM505029; *HuIPMS2*, OM505030; *HuIPMS3*, OM505031.

Conflicts of Interest: The authors declare no conflict of interest.

References

1. Yin, X.; Li, J.H.; Shin, H.D.; Du, G.C.; Liu, L.; Chen, J. Metabolic engineering in the biotechnological production of organic acids in the tricarboxylic acid cycle of microorganisms: Advances and prospects. *Biotechnol. Adv.* **2015**, *33*, 830–841. [\[CrossRef\]](#) [\[PubMed\]](#)
2. Batista-Silva, W.; Nascimento, V.L.; Medeiros, D.B.; Nunes-Nesi, A.; Ribeiro, D.M.; Zsögön, A.; Araújo, W.L. Modifications in organic acid profiles during fruit development and ripening: Correlation or causation? *Front Plant Sci.* **2018**, *9*, 1689. [\[CrossRef\]](#) [\[PubMed\]](#)
3. Chen, F.X.; Liu, X.H.; Chen, L.S. Developmental changes in pulp organic acid concentration and activities of acid-metabolising enzymes during the fruit development of two loquat (*Eriobotrya japonica* Lindl.) cultivars differing in fruit acidity. *Food Chem.* **2009**, *114*, 657–664. [\[CrossRef\]](#)
4. Ma, B.Q.; Yuan, Y.Y.; Gao, M.; Li, C.Y.; Ogutu, C.; Li, M.J.; Ma, F.W. Determination of predominant organic acid components in *Malus* species: Correlation with apple domestication. *Metabolites* **2018**, *8*, 74. [\[CrossRef\]](#)
5. Sha, S.F.; Li, J.C.; Wu, J.; Zhang, S.L. Changes in the organic acid content and related metabolic enzyme activities in developing ‘Xinping’ pear fruit. *Afr. J. Agric. Res.* **2011**, *6*, 3560–3567.
6. Hulme, A.C. A New Hydroxy-acid in the Peel of Apple Fruits. *Nature* **1953**, *172*, 346. [\[CrossRef\]](#)
7. Sugimoto, N.; Engelgau, P.; Jones, A.D.; Song, J.; Beaudry, R. Citramalate synthase yields a biosynthetic pathway for isoleucine and straight- and branched-chain ester formation in ripening apple fruit. *Proc. Natl. Acad. Sci USA* **2021**, *118*, e2009988118. [\[CrossRef\]](#)
8. Frantom, P.A. Structural and functional characterization of alpha-isopropylmalate synthase and citramalate synthase, members of the LeuA dimer superfamily. *Arch. Biochem. Biophys.* **2012**, *519*, 202–209. [\[CrossRef\]](#)
9. Hulme, A.C.; Woollorton, L.S.C. Determination and isolation of the non-volatile acids of pome fruits and a study of acid changes in apples during storage. *J. Sci. Food Agric.* **1958**, *9*, 150–158. [\[CrossRef\]](#)
10. Howell, D.M.; Xu, H.; White, R.H. (R)-citramalate synthase in methanogenic archaea. *J. Bacteriol.* **1999**, *181*, 331–333. [\[CrossRef\]](#)
11. Johnson, D.W.; Eastham, G.R.; Poliakoff, M.; Huddle, T.A. Method of Producing Arcylic and Methacrylic Acid. U.S. Patent 8,933,179, 13 January 2015.
12. Webb, J.; Springthorpe, V.; Rossoni, L.; Minde, D.P.; Langer, S.; Walker, H.; Alstrom-Moore, A.; Larson, T.; Lilley, K.; Eastham, G.; et al. Systems analyses reveal the resilience of *Escherichia coli* physiology during accumulation and export of the nonnative organic acid citramalate. *Msystems* **2019**, *4*, e00187-19. [\[CrossRef\]](#) [\[PubMed\]](#)

13. Webb, J.P.; Arnold, S.A.; Baxter, S.; Hall, S.J.; Eastham, G.; Stephens, G. Efficient bio-production of citramalate using an engineered *Escherichia coli* strain. *Microbiology* **2018**, *164*, 133–141. [[CrossRef](#)]
14. Zhang, K.C.; Woodruff, A.P.; Xiong, M.; Zhou, J.; Dhande, Y.K. A synthetic metabolic pathway for production of the platform chemical isobutyric acid. *ChemSusChem* **2011**, *4*, 1068–1070. [[CrossRef](#)] [[PubMed](#)]
15. Hossain, A.H.; Hendriks, A.; Punt, P.J. Identification of novel citramalate biosynthesis pathways in *Aspergillus niger*. *Fungal Biol. Biotechnol.* **2019**, *6*, 19. [[CrossRef](#)] [[PubMed](#)]
16. Fujimoto, Y.; Yadav, J.S.; Sih, C.J. (S)-citramalic acid, a useful chiral synthon for the synthesis of 15-deoxy-16(S)-hydroxy-16-methylprostaglandins. *Tetrahedron Lett.* **1980**, *21*, 2481–2482. [[CrossRef](#)]
17. Wilkes, J.B.; Wall, R.G. Citric Acid and Citramalic Acid Preparation. U.S. Patent 4,022,823, 10 May 1977.
18. Takao, Y.; Takahashi, T.; Yamada, T.; Goshima, T.; Isogai, A.; Sueno, K.; Fujii, T.; Akao, T. Characteristic features of the unique house sake yeast strain *Saccharomyces cerevisiae* Km67 used for industrial sake brewing. *J. Biosci. Bioeng.* **2018**, *126*, 617–623. [[CrossRef](#)] [[PubMed](#)]
19. Le Bellec, F.; Vaillant, F. Pitahaya (pitaya) (*Hylocereus* spp.). In *Postharvest Biology and Technology of Tropical and Subtropical Fruits*; Woodhead Publishing: Cambridge, UK, 2011; pp. 247–273e. ISBN 978-0-85709-090-4.
20. Zhang, Z.K.; Xing, Y.M.; Ramakrishnan, M.; Chen, C.B.; Xie, F.F.; Hua, Q.Z.; Chen, J.Y.; Zhang, R.; Zhao, J.T.; Hu, G.B.; et al. Transcriptomics-based identification and characterization of genes related to sugar metabolism in ‘Hongshuijing’ pitaya. *Hortic. Plant J.* **2021**; in press. [[CrossRef](#)]
21. Hua, Q.Z.; Chen, C.B.; Tel Zur, N.; Wang, H.C.; Wu, J.Y.; Chen, J.Y.; Zhang, Z.K.; Zhao, J.T.; Hu, G.B.; Qin, Y.H. Metabolomic characterization of pitaya fruit from three red-skinned cultivars with different pulp colors. *Plant Physiol. Biochem.* **2018**, *126*, 117–125. [[CrossRef](#)]
22. Wu, Y.W.; Xu, J.; Shi, M.Y.; Han, X.M.; Li, W.Y.; Zhang, X.W.; Wen, X.P. Pitaya: A potential plant resource of citramalic acid. *CyTA-J. Food* **2020**, *18*, 249–256. [[CrossRef](#)]
23. Hu, Z.; Wang, H.; Hu, G.B. Measurement of sugars, organic acids and vitamin C in litchi fruit by performance liquid chromatography. *J. Fruit Sci.* **2005**, *22*, 582–585.
24. Chen, C.J.; Chen, H.; Zhang, Y.; Thomas, H.R.; Frank, M.H.; He, Y.H.; Xia, R. TBtools: An integrative toolkit developed for interactive analyses of big biological data. *Mol. Plant* **2020**, *13*, 1194–1202. [[CrossRef](#)]
25. Chen, C.B.; Wu, J.Y.; Hua, Q.Z.; Tel-Zur, N.; Xie, F.F.; Zhang, Z.K.; Chen, J.Y.; Zhang, R.; Hu, G.B.; Zhao, J.T.; et al. Identification of reliable reference genes for quantitative real-time PCR normalization in pitaya. *Plant Methods* **2019**, *15*, 70. [[CrossRef](#)]
26. Livak, K.J.; Schmittgen, T.D. Analysis of relative gene expression data using real-time quantitative PCR and the $2^{-\Delta\Delta C_T}$ method. *Methods* **2001**, *25*, 402–408. [[CrossRef](#)]
27. Fan, X.G.; Zhao, H.D.; Wang, X.M.; Cao, J.K.; Jiang, W.B. Sugar and organic acid composition of apricot and their contribution to sensory quality and consumer satisfaction. *Sci. Hortic.* **2017**, *225*, 553–560. [[CrossRef](#)]
28. Minamikawa, M.F.; Nonaka, K.; Kaminuma, E.; Kajiyama-Kanegae, H.; Onogi, A.; Goto, S.; Yoshioka, T.; Imai, A.; Hamada, H.; Hayashi, T.; et al. Genome-wide association study and genomic prediction in citrus: Potential of genomics-assisted breeding for fruit quality traits. *Sci. Rep.* **2017**, *7*, 4721. [[CrossRef](#)]
29. Ramadan, N.S.; Wessjohann, L.A.; Mocan, A.; Vodnar, D.C.; El-Sayed, N.H.; El-Toumy, S.A.; Mohamed, D.A.; Aziz, Z.A.; Ehrlich, A.; Farag, M.A. Nutrient and sensory metabolites profiling of *Averrhoa carambola* L. (Starfruit) in the context of its origin and ripening stage by GC/MS and chemometric analysis. *Molecules* **2020**, *25*, 2423. [[CrossRef](#)]
30. Xu, J.D.; Yan, J.J.; Li, W.J.; Wang, Q.Y.; Wang, C.X.; Guo, J.X.; Geng, D.L.; Guan, Q.M.; Ma, F.W. Integrative analyses of widely targeted metabolic profiling and transcriptome data reveals molecular insight into metabolomic variations during apple (*Malus domestica*) fruit development and ripening. *Int. J. Mol. Sci.* **2020**, *21*, 4797. [[CrossRef](#)] [[PubMed](#)]
31. Lee, K.M.; Oh, T.J.; Kim, S.H.; Kim, H.Y.; Chung, H.; Min, D.S.; Auh, J.H.; Lee, H.J.; Lee, J.; Choi, H.K. Comprehensive metabolic profiles of mulberry fruit (*Morus alba* Linnaeus) according to maturation stage. *Food Sci. Biotechnol.* **2016**, *25*, 1035–1041. [[CrossRef](#)] [[PubMed](#)]
32. Qiu, G.L.; Zhuang, Q.G.; Li, Y.F.; Li, S.Y.; Chen, C.; Li, Z.H.; Zhao, Y.Y.; Yang, Y.; Liu, Z.B. Correlation between fruit weight and nutritional metabolism during development in CPPU-treated *Actinidia chinensis* ‘Hongyang’. *PeerJ* **2020**, *8*, e9724. [[CrossRef](#)]
33. Wu, X.H.; Tovilla-Coutino, D.B.; Eiteman, M.A. Engineered citrate synthase improves citramalic acid generation in *Escherichia coli*. *Biotechnol. Bioeng.* **2020**, *117*, 2781–2790. [[CrossRef](#)]
34. Walker, R.P.; Paoletti, A.; Leegood, R.C.; Famiani, F. Phosphorylation of phosphoenolpyruvate carboxykinase (PEPCK) and phosphoenolpyruvate carboxylase (PEPC) in the flesh of fruits. *Plant Physiol. Biochem.* **2016**, *108*, 323–327. [[CrossRef](#)]
35. Yao, Y.X.; Li, M.; Zhai, H.; You, C.X.; Hao, Y.J. Isolation and characterization of an apple *Cytosolic malate dehydrogenase* gene reveal its function in malate synthesis. *J. Plant Physiol.* **2011**, *168*, 474–480. [[CrossRef](#)] [[PubMed](#)]
36. Yao, Y.X.; Dong, Q.L.; Zhai, H.; You, C.X.; Hao, Y.J. The functions of an apple *Cytosolic malate dehydrogenase* gene in growth and tolerance to cold and salt stresses. *Plant Physiol. Biochem.* **2011**, *49*, 257–264. [[CrossRef](#)]
37. Chen, Q.Q.; Wang, B.P.; Ding, H.Y.; Zhang, J.; Li, S.C. Review: The role of NADP-malic enzyme in plants under stress. *Plant Sci.* **2019**, *281*, 206–212. [[CrossRef](#)] [[PubMed](#)]
38. Kou, X.H.; Wang, S.; Zhang, Y.; Guo, R.Z.; Wu, M.S.; Chen, Q.; Xue, Z.H. Effects of chitosan and calcium chloride treatments on malic acid-metabolizing enzymes and the related gene expression in post-harvest pear cv. ‘Huang guan’. *Sci. Hortic.* **2014**, *165*, 252–259. [[CrossRef](#)]

39. Gao, L.; Zhao, S.J.; Lu, X.Q.; He, N.; Zhu, H.J.; Dou, J.L.; Liu, W.G. Comparative transcriptome analysis reveals key genes potentially related to soluble sugar and organic acid accumulation in watermelon. *PLoS ONE* **2018**, *13*, e0190096. [[CrossRef](#)] [[PubMed](#)]
40. Zhang, X.X.; Wei, X.X.; Ali, M.M.; Rizwan, H.M.; Li, B.Q.; Li, H.; Jia, K.J.; Yang, X.L.; Ma, S.F.; Li, S.J.; et al. Changes in the content of organic acids and expression analysis of citric acid accumulation-related genes during fruit development of yellow (*Passiflora edulis* F. Flavicarpa) and purple (*Passiflora edulis* F. Edulis) passion fruits. *Int. J. Mol. Sci.* **2021**, *22*, 5765. [[CrossRef](#)] [[PubMed](#)]
41. Leroy, B.; De Meur, Q.; Moulin, C.; Wegria, G.; Ruddy, W. New insight into the photoheterotrophic growth of the isocitrate lyase-lacking purple bacterium *Rhodospirillum rubrum* on acetate. *Microbiology* **2015**, *161*, 1061–1072. [[CrossRef](#)]
42. Atsumi, S.; Liao, J.C. Directed evolution of *Methanococcus jannaschii* citramalate synthase for biosynthesis of 1-propanol and 1-butanol by *Escherichia coli*. *Appl. Environ. Microbiol.* **2008**, *74*, 7802–7808. [[CrossRef](#)]
43. Wu, X.H.; Eiteman, M.A. Synthesis of citramalic acid from glycerol by metabolically engineered *Escherichia coli*. *J. Ind. Microbiol. Biotechnol.* **2017**, *44*, 1483–1490. [[CrossRef](#)]
44. Textor, S.; de Kraker, J.W.; Hause, B.; Gershenzon, J.; Tokuhisa, J. MAM3 catalyzes the formation of all aliphatic glucosinolate chain lengths in *Arabidopsis*. *Plant Physiol.* **2007**, *144*, 60–71. [[CrossRef](#)]